

A. Bode · W. Salvenmoser · K. Nimeth ·
M. Mahlknecht · Z. Adamski
R. M. Rieger · R. Peter · P. Ladurner

Immunogold-labeled S-phase neoblasts, total neoblast number, their distribution, and evidence for arrested neoblasts in *Macrostomum lignano* (Platyhelminthes, Rhabditophora)

Received: 4 May 2005 / Accepted: 28 February 2006
© Springer-Verlag 2006

Abstract Neoblasts in Platyhelminthes are the only cells to proliferate and differentiate into all cell types. In *Macrostomum lignano*, the incorporation of 5'-bromo-2'-deoxyuridine (BrdU) in neoblasts confirmed the distribution of S-phase cells in two lateral bands. BrdU labeling for light and for transmission electron microscopy (TEM) identified three populations of proliferating cells: somatic neoblasts located between the epidermis and gastrodermis (mesodermal neoblasts), neoblasts located within the gastrodermis (gastrodermal neoblasts), and gonadal S-phase cells. In adults, three stages of mesodermal neoblasts (2, 2–3, and 3) defined by their ultrastructure were found. Stage 1 neoblasts were only seen in hatchlings. These stages either were phases within the S-phase of one neoblast pool or were subsequent stages of differentiating

neoblasts, each with its own cell cycle. Regular TEM and immunogold labeling provided the basis for calculating the total number of neoblasts and the ratio of labeled to non-labeled neoblasts. Somatic neoblasts represented 6.5% of the total number of cells. Of these, 27% were labeled in S-phase. Of this fraction, 33% were in stage 2, 46% in stage 2–3, and 21% in stage 3. Immunogold labeling substantiated results concerning the differentiation of neoblasts into somatic cells. Non-labeled stage 2 neoblasts were present, even after a 2-week BrdU exposure. Double labeling of mitoses and FMRF-amide revealed a close spatial relationship of mesodermal neoblasts with the nervous system. Immunogold-labeled sections showed that nearly 70% of S-phase cells were in direct contact or within 5 µm from nerve cords.

P.L. was the recipient of an APART fellowship (no. 10841) from the Austrian Academy of Sciences, and Z.A. was the recipient of an Ernst Mach fellowship from the ÖAD. This work was also supported by FWF grants 15204 and 16618 to R.M.R. and P18099 to P.L.

Keywords Stem cells · BrdU · Immunogold · Electron microscopy · Planarian · *Macrostomum lignano* (Platyhelminthes)

A. Bode · W. Salvenmoser · K. Nimeth · M. Mahlknecht ·
R. M. Rieger · P. Ladurner (✉)
Institute of Zoology and Limnology, University of Innsbruck,
Technikerstrasse 25,
6020 Innsbruck, Austria
e-mail: peter.ladurner@uibk.ac.at

Z. Adamski
Faculty of Biology, Institute of Experimental Biology, Electron
Microscope Laboratory, Adam Mickiewicz University,
Ul. Grunwaldzka 6,
60-780 Poznań, Poland

Z. Adamski
Faculty of Biology, Institute of Experimental Biology,
Department of Animal Physiology
Adam Mickiewicz University,
Ul. Fredry 10,
61-701 Poznań, Poland

R. Peter
Department of Cell Biology, University of Salzburg,
Hellbrunnerstrasse 34,
5020 Salzburg, Austria

Introduction

Stem cells are defined by their capacity both for self-renewal and for generating differentiated progeny (Morrison et al. 1997). The stem cell system of the Platyhelminthes is special within the Animal Kingdom because its cells may be totipotent (Baguña 1981; Shibata et al. 1999; Ladurner et al. 2000; Gschwentner et al. 2001; Saló and Baguña 2002; Nimeth et al. 2004). The “stem cells”, referred to as “neoblasts” (for general references, see Brøndsted 1969; Baguña 1998), probably include successions of self-renewing “true” stem cells and several generations of progenitor cells with progressively restricted proliferation potential (for general characteristics of stem cell strategies, see Peter et al. 2004). So far, neoblasts have been identified as the only mitotically active cells in Platyhelminthes and are therefore the only possible source for all differentiated cells during growth, tissue maintenance (cell renewal), and regeneration (e.g., Sauzin–Monnot 1973; Hori 1997;

Ladurner et al. 2000; Newmark and Sánchez Alvarado 2000; Peter et al. 2001; Saló and Bagaña 2002; Sánchez Alvarado et al. 2002; Reuter and Kreshchenko 2004).

At the light-microscopic level, somatic neoblasts of the free-living Platyhelminthes (“Turbellaria”) appear as small ovoid basophilic cells with a high nucleocytoplasmic ratio (e.g., Brøndsted 1969; Bagaña and Romero 1981). They are mainly located in the tissues filling the space between the epidermis and gastrodermis; a few occur in the gastrodermis (Palmberg 1990; Rieger et al. 1991; Ehlers 1995; Hori 1997; Rieger et al. 1999; Ladurner et al. 2000; Newmark and Sánchez Alvarado 2000). This characterization also applies to the parasitic platyhelminths (e.g., Gustafsson 1976, 1990; Ehlers 1995). We refer to these two populations of somatic neoblasts as “mesodermal” when they are located between the epidermis and gastrodermis, and “gastrodermal” when they lie within the gastrodermis.

It has been stressed (see Hay and Coward 1975; Rieger et al. 1999) that electron microscopy should be used to classify the different stages of neoblasts and to distinguish them from early stages of differentiating cells. At the ultrastructural level, somatic neoblasts contain a large nucleus with a prominent nucleolus and a typical heterochromatin pattern, scanty cytoplasm with free ribosomes, mitochondria, and occasionally endoplasmic reticulum, depending on the stage of cytoplasmic differentiation (see also Pedersen 1959; Palmberg 1990; Morita 1995; Hori 1997; Hori et al. 1999; Gschwentner et al. 2001). The similarity of the nuclear fine structure of oogonia, spermatogonia, and somatic neoblasts has been emphasized earlier (Rieger et al. 1999).

In *Macrostomum hystricinum marinum*, we have distinguished three stages of neoblasts on the basis of their cytoplasmic and nuclear organization (Rieger et al. 1999). Only free ribosomes and scattered mitochondria occur in the cytoplasm of stage 1 and stage 2 neoblasts, comparable to the “classical” planarian neoblast (except for the lack of chromatoid bodies; e.g., Pedersen 1959; Sauzin-Monnot 1973; Hay and Coward 1975; Hori 1997; Hori and Kishida 1998). Heterochromatin is distributed in the nucleus in isolated clumps (0.2 μm in size) in a characteristic speckled pattern; it is rarely seen at the nuclear envelope. The heterochromatin clumps in stage 2 are more often connected to each other. At stage 3, larger heterochromatin strands appear in the nucleoplasm and adjacent to the nuclear margins. In addition, cells in stage 3 have been reported with rough endoplasmic reticulum and may exhibit a dictyosome indicating the beginning of cytoplasmic differentiation. It is not clear whether these three stages reflect different phases during the cell cycle of one neoblast population, or whether they represent different sequential subpopulations of neoblasts, each with its own cell cycle.

We have studied the neoblast system of some of the most basal rhabditophoran platyhelminth taxa by using the incorporation of the thymidine analogue 5-bromo-2'-

deoxyuridine (BrdU) into DNA during S-phase, by dissolving BrdU in the sea-water cultivating medium (for details, see Ladurner et al. 2000; Gschwentner et al. 2001). Tritiated thymidine has been used for the same purpose in fresh-water microturbellarians (Palmberg and Reuter 1983; Palmberg 1986, 1990) and in parasitic flatworms (Neodermata; see Gustafsson 1990; Smith and McKerr 2000; Willms et al. 2001; Reuter and Kreshchenko 2004). In planarians, attempts to incorporate BrdU have been unsuccessful (Best et al. 1965) until recently, when incorporation of BrdU into neoblasts has been achieved by feeding and microinjection (Newmark and Sánchez Alvarado 2000).

Quantification of neoblasts is still problematic (see references in Ladurner et al. 2000; Newmark and Sánchez Alvarado 2000; Peter et al. 2001; Gschwentner et al. 2001). From maceration experiments in planarians, the percentage reported varies from 20%-35% neoblasts of total cell counts in *Schmidtea mediterranea* and in *Dugesia tigrina* (Bagaña and Romero 1981) up to 44% neoblasts in *Dugesia tahitiensis* (Peter 1995, 2001). In the Acoela, the same technique has so far revealed that about 15% of all cells are S-phase neoblasts (Gschwentner et al. 2001).

In *Macrostomum lignano*, Ladurner et al. (2000) have found approximately 2% of all cells to be in S-phase after a 30-min incubation with BrdU. Of course, this comprises only a fraction of the total number of neoblasts, which is still unknown. For an estimate of the total number of neoblasts and the relative numbers of the three neoblast stages in *M. lignano*, we have used, in this study, a 30-min BrdU pulse, followed by immunogold labeling, to demonstrate S-phase neoblasts and transmission electron microscopy (TEM) to identify non-labeled neoblast stages. In addition, continuous BrdU-labeling experiments have been performed to trace the label during cell differentiation and long-term continuous BrdU labeling to seek the presence of unlabeled neoblasts with slow or resting cell cycles. Furthermore, we show the close association of proliferating neoblasts (mitoses) with the nervous system.

Materials and methods

Animals

Cultures of *Macrostomum lignano* (Ladurner et al. 2005), a new species belonging to the *Macrostomum tuba* clade (Platyhelminthes), were reared in Petri dishes on the diatom *Nitzschia curvilineata* (Rieger et al. 1988; Schärer and Ladurner 2003; for the identification of this species, see Ladurner et al. 2000). Cultures were raised in a chamber at 20°C with 50% humidity and a photoperiod of 14 h light and 10 h dark. Adult animals used for the experiments were fed for 1 week continuously and then starved for 2 days prior to the experiments in order to remove diatoms.

Labeling of S-phase cells with BrdU and determination of ultrastructural stages and neoblast numbers

We performed different sets of experiments for light microscopy and for electron microscopy: (1) pulses of 5 mM BrdU in artificial sea water (ASW) for 30 min, and (2) continuous exposure to 50 μ M BrdU for 1 and 2 weeks. Specimens were kept in the dark, with feeding and a change of medium after 1 week.

Four different body regions (Fig. 1), each with a width of 30–40 μ m in adult animals, were subjected for S-phase nuclei measurement: the region close to the caudal end of the gut (region 1), the region in the gut behind the gonads (region 2), the region within the male and female gonads (region 3), and the region anterior to the gonads caudal to the mouth and pharynx (region 4). Neoblast numbers were enumerated only in body regions 1 and 2 by using ultra-thin immunogold sections (see below). To avoid counting neoblast nuclei twice, we defined the distance between ultra-thin sections as more than 8 μ m, a distance just larger than the maximum diameter of neoblast nuclei observed. To count neoblasts and to determine the ratio between S-phase and non-S-phase neoblasts after a 30-min BrdU pulse, we investigated 22 grids, each with 2–4 sections from both region 1 and region 2 of three different animals. All sections were examined with a Zeiss 902 transmission electron microscope. Sections were studied by using digital images; for the resolution of small cytological details, regular prints were employed.

Light microscopy

After BrdU exposure, animals were relaxed in 1:1 ASW-MgCl₂.6H₂O (7.14 %) for 20 min, fixed either in 4% paraformaldehyde (PFA) or glutaraldehyde in phosphate-buffered saline (PBS, pH 7.4) containing 10% sucrose for 60 min at room temperature (RT), and washed in PBS (3 \times 10 min). Specimens were treated with 0.15 μ g/ml Protease XIV (Sigma) at 37°C for 30 min, followed by incubation in 0.1 N HCl for 10 min, on ice. They were then transferred to 2 N HCl for 60 min at 37°C to denature DNA, washed in PBS (3 \times 10 min), and incubated in blocking solution “BSA-T” consisting of PBS with 0.1% Triton X-100, 1% bovine serum albumin (BSA) for 1 h. Primary antibody (mouse-anti-BrdU; Sigma; 1:1,000 in

BSA-T)) was applied at 4°C overnight, followed by blocking of endogenous peroxidase for later visualization with horseradish peroxidase (HRP)/diaminobenzidine (DAB) in freshly prepared 1% H₂O₂. After being washed in PBS (3 \times 10 min), specimens were incubated in secondary fluorescein isothiocyanate (FITC)-conjugated goat-anti-mouse antibody (Dako; 1:400 in BSA-T), washed in PBS (3 \times 10 min), and incubated in HRP-conjugated rabbit-anti-FITC antibody (Dako; 1:300 in BSA-T) for 1 h at RT. Animals were stained with peroxidase reagent (Dako-Liquid DAB) for few minutes at RT under visual control. Specimens were mounted in Gel-Mount (Biomedica) and examined with a Reichert POLYVAR microscope. Some animals were dehydrated and embedded in Spurr’s low viscosity resin for the production of semi-thin serial sections.

Electron microscopy

To detect the incorporation of BrdU by TEM, we used a standard immunogold-technique according to Hacker et al. (1996). After BrdU treatment, animals were relaxed in MgCl₂.6H₂O (7.14%), fixed in 2.5% glutaraldehyde in 0.1 M cacodylate buffer (pH 7.2) containing 10% sucrose (1 h), postfixed with 1% osmium tetroxide in 0.1 M cacodylate buffer (1 h), dehydrated in a standard acetone series, and embedded in Spurr’s low viscosity resin (Spurr 1969). Ultra-thin sections were cut with a Reichert Ultracut UCT, mounted on gold slotgrids, etched with freshly prepared 3% H₂O₂ (10 min), and incubated in 2 N HCl (5 min) to denature DNA. Sections were treated with 1% BSA in 0.1 M PBS for 15 min, followed by incubation in 0.1% cold-water-fish gelatine (FG/BSA in 0.1 M PBS and 1% BSA) for 5 min. Primary antibody (mouse-anti-BrdU; Sigma; 1:6,000 in FG/BSA) was applied at 4°C overnight. After washing steps, a secondary gold-conjugated goat-anti-mouse antibody (10 nm gold, 1:40 or 1:60 in FG/BSA; British Bio Cell) was applied for 1 h at RT. Sections were double stained with uranyl acetate and lead citrate and examined with a Zeiss 902 transmission electron microscope.

For immunogold labeling of S-phase neoblasts in hatchlings of *Macrostomum lignano*, fixation according to Eisenman and Alfert (1982) and a modified protocol for immunostaining were used. After BrdU treatment, animals were relaxed, fixed, and embedded as stated above. Primary antibody (mouse-anti-BrdU; Roche, 1:2,000 in FG/BSA) was applied at RT overnight. After washing steps, a secondary gold-conjugated goat-anti-mouse antibody (10 nm gold, 1:40 or 1:60 in FG/BSA; British Bio Cell) was applied for 2 h at RT. Sections were double stained with uranyl acetate and lead citrate and examined with a Zeiss 902 transmission electron microscope.

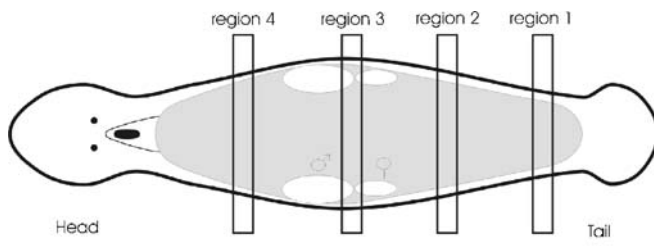


Fig. 1 Representation of *Macrostomum lignano* with the four regions taken for the measurement of S-phase nuclei (region 1–4) and for alternating semi-thin and ultra-thin sections (region 1, 2)

For each staining procedure, negative controls were carried out by omitting the primary antibody and showed no background staining.

Double labeling of mitoses (anti-phos-H3) and nervous system (anti-FMRF-amide)

Relaxation, fixation, and blocking were performed as described above. Specimens were incubated in primary anti-FMRF-amide (Incstar Corporation, 1:1,000 in BSA-T) at 4°C overnight, washed in PBS (3×10 min) and incubated in secondary tetramethylrhodamine-isothiocyanate-conjugated swine anti-rabbit antibody (Dako; 1:150 in BSA-T). After being washed in PBS (3×10 min), animals were incubated in anti-phos-H3 (Upstate Biotechnology; 1:300 in BSA-T) at 4°C overnight, washed in PBS (3×10 min), incubated in secondary FITC-conjugated swine anti-rabbit antibody (Dako; 1:150 in BSA-T) for 60 min at RT, washed again in PBS (3×10 min), mounted in Vectashield, and observed with a Reichert POLYVAR epifluorescence microscope or a confocal Zeiss 510 laser scanning microscope.

Results

Neoblast populations

In *M. lignano*, three different populations of S-phase cells were labeled after a 30-min BrdU pulse. Mesodermal neoblasts constituted the majority of all S-phase neoblasts (see below) and were distributed in bands along the lateral sides of the animal (Fig. 2a). Their position between epidermis and gastrodermis was determined by light microscopy (Fig. 2b; for TEM, see Fig. 6a). Mesodermal S-phase cells were lacking anterior to the eyes in the entire rostrum and to a variable extent in the tail plate, behind the caudal ganglion (Fig. 2a).

A second population, viz., gastrodermal neoblasts, were distributed in the gastrodermis in a basiepithelial position (Fig. 2b, see also Fig. 6a) and represent a small fraction (some of the cells seen in Fig. 2a as being scattered between the lateral bands of mesodermal neoblasts).

A third population could be identified in the testis and the ovary (Fig. 2c). Such “gonadal” S-phase cells represented approximately 0.4% (calculated after Ladurner et al. 2000) of the total cell number. The majority were found in the germinal epithelium enclosing the gonads. The

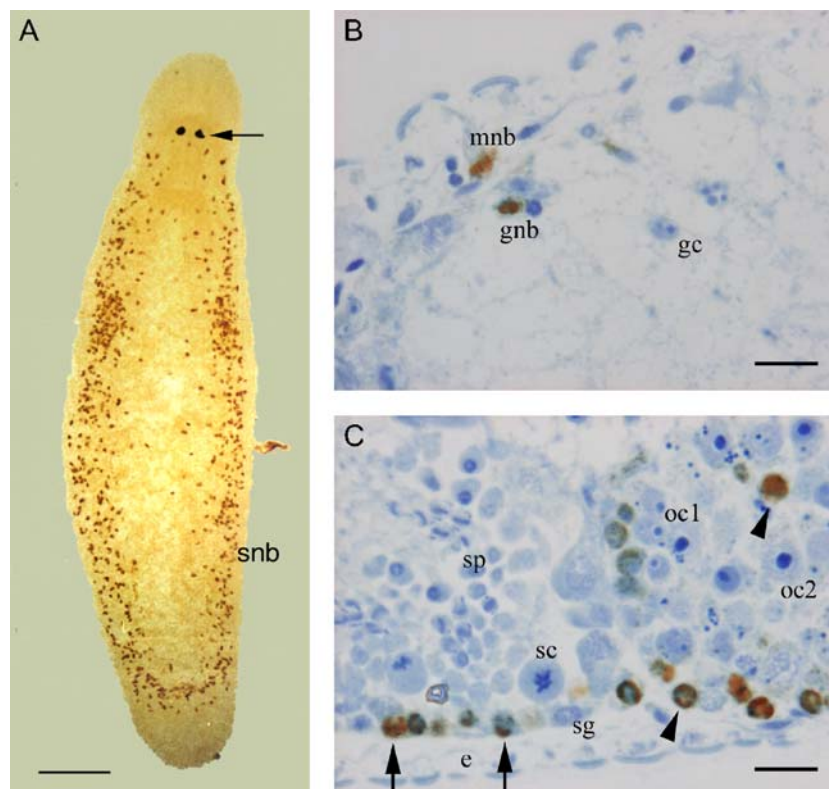


Fig. 2 **a** Light-microscopic image of whole-mount of adult *Macrostomum lignano* after a 30-min BrdU pulse visualized with DAB (arrow level of eyes). Note the S-phase-free area in front of the eyes. Somatic neoblasts (*snb*) occur in bands along the lateral side of the animal. Bar 50 μ m. **b** Semi-thin oblique cross section in dorsolateral position of an adult specimen after a 30-min BrdU pulse; note the mesodermal neoblast (*mnb*) and gastrodermal neoblast (*gnb*) in S-phase in a basiepithelial position (*gc*

differentiated gut cell closer to lumen). Bar 10 μ m. **c** Semi-thin sagittal section (left anterior) of adult specimen after a 30-min BrdU pulse showing spermatogenesis in the testis (left) and oogenesis in the ovary (right). Labeled (arrows) and non-labeled (*sg*) spermatogonia are located at the outer rim of the testis. Spermatocytes (*sc*) and spermatids (*sp*) are present toward the lumen. In the ovary, S-phase oogonia (arrowheads), oocytes 1 (*oc1*, and oocytes 2 (*oc2*) can be distinguished (*e* epidermis). Bar 10 μ m

number of S-phase cells in the gonads was highly affected by the feeding conditions (Schärer et al. 2004).

Neoblast differentiation and observation of slow-cycling neoblasts

After 1 week of continuous BrdU exposure, we found gold labeling in various kinds of differentiating and differentiated cell types (e.g., epidermal cells, epidermal gland cells, gastrodermal cells). The differentiation and migration of neoblasts could be monitored after 2 weeks of continuous BrdU labeling (Fig. 3a,b) and in BrdU pulse-chase experiments (data not shown). We confirmed earlier experiments (Ladurner et al. 2000; Nimeth et al. 2002, 2004) concerning the fast renewal of epidermal cells. These were easily observed, even in whole-mounts, at the tail plate (Fig. 3a) and were demonstrated with immunogold labeling (Fig. 3b). In analyses of mature epidermal cells, the gold label was located exclusively in the condensed chromatin areas (Fig. 3b).

Thin sections after continuous BrdU exposure for 1 week (2 specimen, 16 grids) or 2 weeks (2 specimen, 16 grids) exhibited a small number of non-labeled stage 2 neoblasts (Fig 3c). We quantified only the 2-week BrdU exposure experiment: neoblasts were counted in one specimen cross-sectioned over a distance of 9 μm ; this revealed one unlabeled neoblast and 13 labeled neoblasts on one lateral side of the animal. The other specimen was longitudinally sectioned and contained mesodermal tissue for a distance of 180 μm . Three unlabeled and 10 labeled neoblasts were found within this section.

Ultrastructural stages of neoblasts

At the ultrastructural level, we concentrated our investigations on mesodermal neoblasts after a 30-min BrdU incubation of adult animals. In adults, mesodermal neoblasts of stage 2 (Figs. 3c, 5a,b), of an intermediate stage 2–3 (Fig. 5c–f), and of stage 3 (Figs. 6c, 7) could be distinguished. The nuclear organization of stage 2 and stage 3 neoblasts compared well with the conditions reported for *M. hystricinum marinum* (Rieger et al. 1999). Most nuclei were elongated (up to 8 μm long, 1.5 μm in diameter; Figs. 3c, 7), and a prominent nucleolus was present in most sections (Figs. 3c, 4, 7). In nuclei of stage 2 neoblasts, condensed chromatin clumps were either separate or formed short strands, and little condensed chromatin was found adjacent to the nuclear envelope (Figs. 3c, 5a,b). Cytoplasm formed a thin layer over the elongated nuclei, with accumulations on both ends of the cell (Figs. 3c, 7). Occasionally, lipid droplets were found (Fig. 4). The cytoplasm of stage 2 neoblasts contained primarily free ribosomes and mitochondria. Small strands of rER were seen sporadically. In stage 3 neoblasts, the condensed chromatin formed thicker strands, whereas individual clumps were seen more rarely (Figs. 6c, 7). In the cytoplasm at this stage, rER was usually visible, in addition

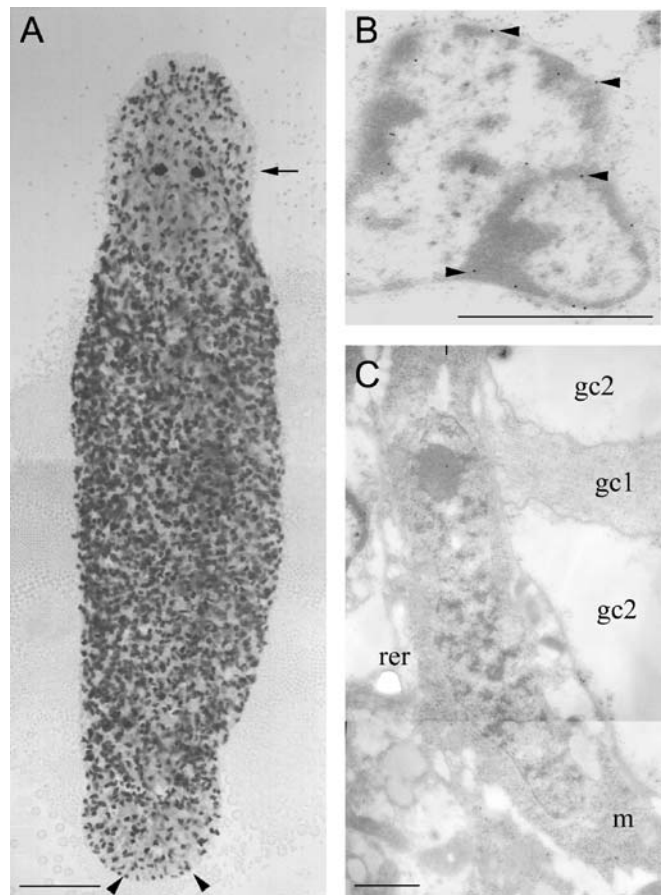


Fig. 3 a Light-microscopic image of whole-mount of adult *M. lignano* after a 7-day continuous BrdU exposure (arrow level of eyes). Note the high number of labeled cells in the rostrum, the median zone, and the tail plate; these must have migrated from the lateral bands to their new positions (arrowheads indicate differentiated epidermal cells). Bar 50 μm . b Immunogold labeling (arrowheads) of a differentiated epidermal cell after 7 days of continuous BrdU exposure. Bar 1 μm . c Immunogold labeling after 14 days of continuous BrdU exposure showing a non-labeled stage 2 neoblast with mitochondria (m) and rough endoplasmic reticulum (rer) in the parenchyma between the musculature and young (gc1) and mature gut cells (gc2). Bar 1 μm

to free ribosomes and mitochondria. Dictyosomes were rarely found. In a number of neoblasts, the distinction from stage 2 was less obvious, and these cells were classified as stage 2–3 (Fig. 5c).

Gold labeling for BrdU in S-phase nuclei was located in areas of condensed chromatin and adjacent areas of dispersed chromatin (Fig. 5b,d). In all thin sections examined, labeled (Figs. 5a–d, 7) and non-labeled neoblasts (Figs. 3c, 6c) always co-occurred (e.g., Fig. 6b).

Neoblast stages showed the following distribution within the 71 S-phase neoblasts found in sections of the selected body regions (Table 1): 0% were stage 1, 33% were stage 2, 46% were stage 2–3, and 21% were stage 3. Among the 264 non-labeled neoblasts enumerated within the selected two body regions, no stage 1 neoblasts were observed, 8% were stage 2 neoblasts, 25% were stage 2–3, and stage 3 neoblasts made up the largest portion of about 67% (Table 1).

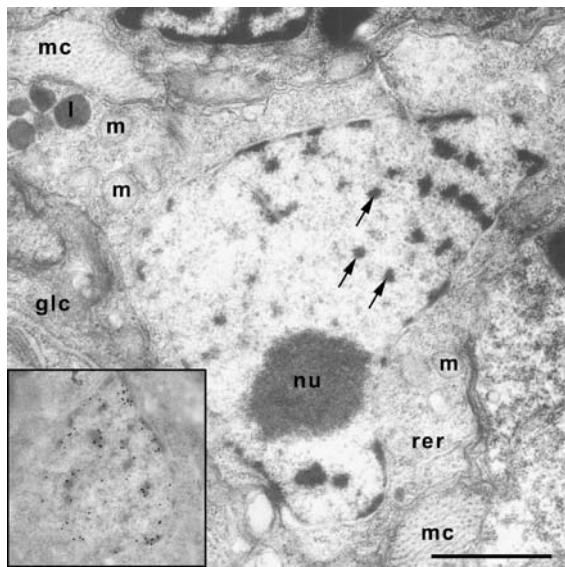


Fig. 4 BrdU-labeled neoblast stage 1 in a hatchling of *M. lignano*. This section was not immunogold labeled for better preservation of the fine structure. Note the isolated spots of condensed chromatin (arrows) and the large nucleolus (*nu*). The cytoplasm contains ribosomes, a little rough endoplasmic reticulum (*rer*), mitochondria (*m*), and some lipid droplets (*l*). Muscle fibers (*mc*) and a gland cell (*glc*) surround the neoblast. *Inset* Consecutive section of the same neoblast nucleus with both condensed and dispersed chromatin having been immunogold-labeled. *Bar* 1 μ m

Calculating the total number of neoblasts

The ability to enumerate non-labeled and labeled somatic neoblasts after a 30-min BrdU pulse in the same specimen has allowed, for the first time, an estimation of the total number of neoblasts in *M. lignano*. The absolute number of somatic S-phase neoblasts is 435 ± 79 for adult animals (Ladurner et al. 2000). After a 30-min BrdU pulse, we have observed approximately 27% labeled neoblasts (71 out of 264 neoblasts; Table 1). From this percentage (27%) and the total number of S-phase neoblasts counted in whole-mounts, we estimate a total number of about 1,600 neoblasts for *M. lignano*. The total number of all cells in adults has been determined as $24,708 \pm 3,831$ (Ladurner et al. 2000). From this, we calculate that approximately 6.5% (1,600 out of 24,708) of all cells are neoblasts.

Table 1 Distribution of the various neoblast stages after a 30-min BrdU pulse

Stages	S-phase neoblasts	Total neoblasts	Non-labeled neoblasts
1	0% (0)	0% (0)	0% (0)
2	33% (23)	14% (38)	8% (15)
2–3	46% (33)	31% (82)	25% (49)
3	21% (15)	55% (144)	67% (129)
All stages	100% (71)	100% (264)	100% (193)

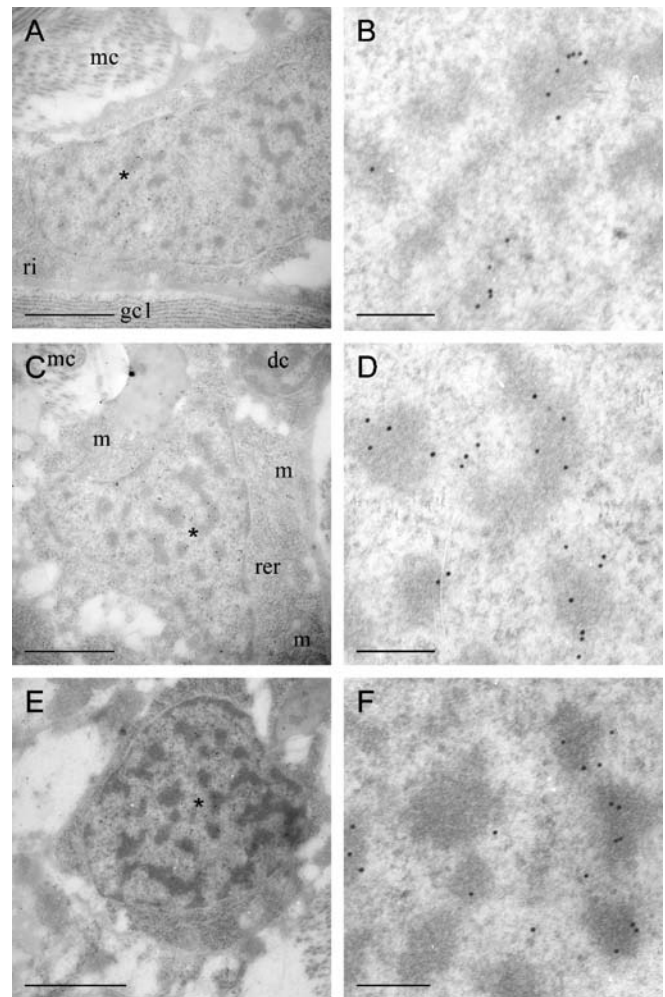


Fig. 5 Immunogold labeling of various mesodermal neoblast stages after a 30-min BrdU pulse. **a** Neoblast stage 2, with typical chromatin pattern, from the parenchyma between body-wall musculature (*mc*) and the gut (*glc*). Cytoplasmic differentiation: note the mitochondria and free ribosomes (*ri*). *Bar* 1 μ m. **b** Higher magnification of **a**. *Bar* 200 nm. **c** Neoblast stage 2–3, with typical chromatin pattern, from the parenchyma. Additional rough endoplasmic reticulum (*rer*) is present at this stage. Compare the chromatin organization of stage 2 (**a**, **b**) and stage 2–3 (**c**, **d**) neoblasts with stage 3 neoblasts and differentiated cells presented in Fig. 7. *Bar* 1 μ m. **d** Higher magnification of **c**. *Bar* 200 nm. **e** Neoblast stage 2–3, with typical chromatin pattern, from the parenchyma. *Bar* 1 μ m. **f** Higher magnification of **e**. *Bar* 200 nm

Relationship of neoblasts and the nervous system

The spatial distribution of S-phase cells after 30-min BrdU exposure supports the existence of links between S-phase neoblasts and the central parts of the nervous system. In double-stained whole-mounts (anti-phos-H3 and anti-FMRF-amide), the great majority of all mitotic figures is clearly located closely attached to the main nerve cords (Fig. 8). Additional mitoses are found near the dorsal and ventral nerve cords, near the intestinal plexus, and the caudal ganglion and at the postpharyngeal commissure. In

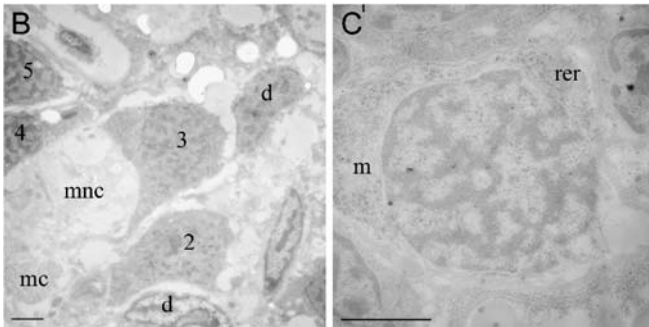
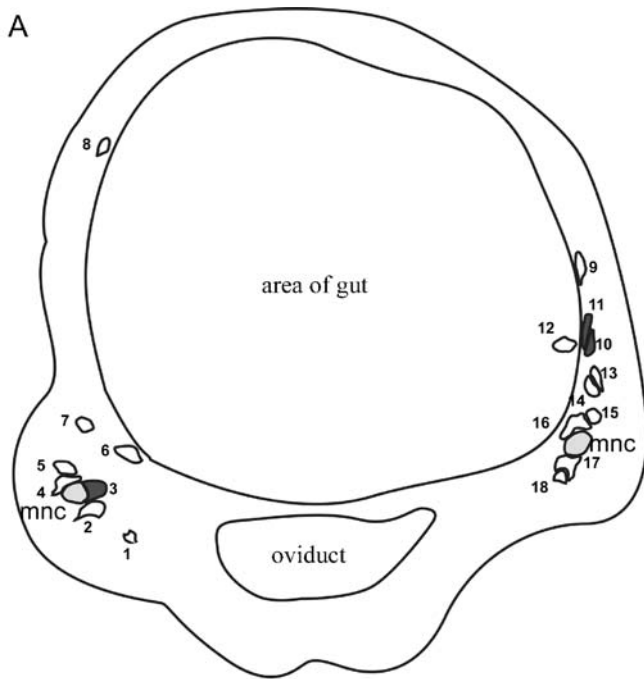


Fig. 6 **a** Representation of a cross section with labeled (*dark gray*) and non-labeled (*white*) neoblasts surrounding the main nerve cord (*mnc*, *light gray*). All neoblasts present in this section are numbered consecutively (1–18). *Number 12* represents a gastrodermal neoblast, whereas all other are mesodermal. **b** Distribution of cells in close vicinity to the main nerve cord (*mnc*) in an immunogold-labeled cross section after a 30-min BrdU pulse (*d* differentiated cell, 2 non-labeled stage 2 neoblast, 3 labeled stage 2 neoblast in direct contact with the main nerve cord, 4, 5 non-labeled stage 3 neoblasts, *mc* musculature). *Numbers* of neoblasts are the same as in **a**. *Bar* 1 μm . **c** Immunogold labeling after a 30-min BrdU pulse showing a non-labeled stage 3 neoblast with mitochondria (*m*) and rough endoplasmic reticulum (*rer*). *Bar* 1 μm

addition, our ultrastructural analysis of sections within the two body regions has revealed that the lateral location of S-phase neoblasts especially is restricted to the vicinity of the main lateral nerve cord (Fig. 6a) and does not extend beyond the ventral and dorsal nerve cords (Fig. 8a). Of the observed 71 S-phase neoblasts, 34% lie directly adjacent to the main nerve cords, and an additional 35% are within a distance of 5 μm from it. From counts of labeled and non-labeled neoblasts, almost 54% are located within a distance of 5 μm from the nerve cord (Fig. 6b).

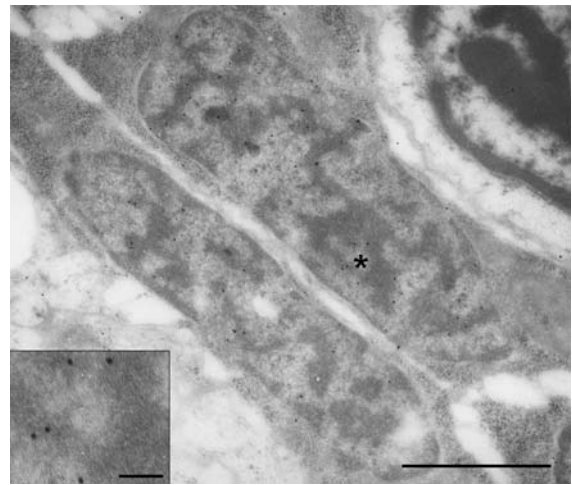


Fig. 7 Regular image of BrdU labeled neoblasts stage 3 at the TEM level. Note the large meandering pattern of condensed chromatin in the nucleus. These two cells are located close to the neoblast stage 2–3 shown in Fig. 5e. The nucleus of differentiated muscle cell lies *top right* (*star* area shown at higher magnification in the *inset*). *Bar* 1 μm . *Inset*: Enlarged area with immunogold label. *Bar* 100 nm

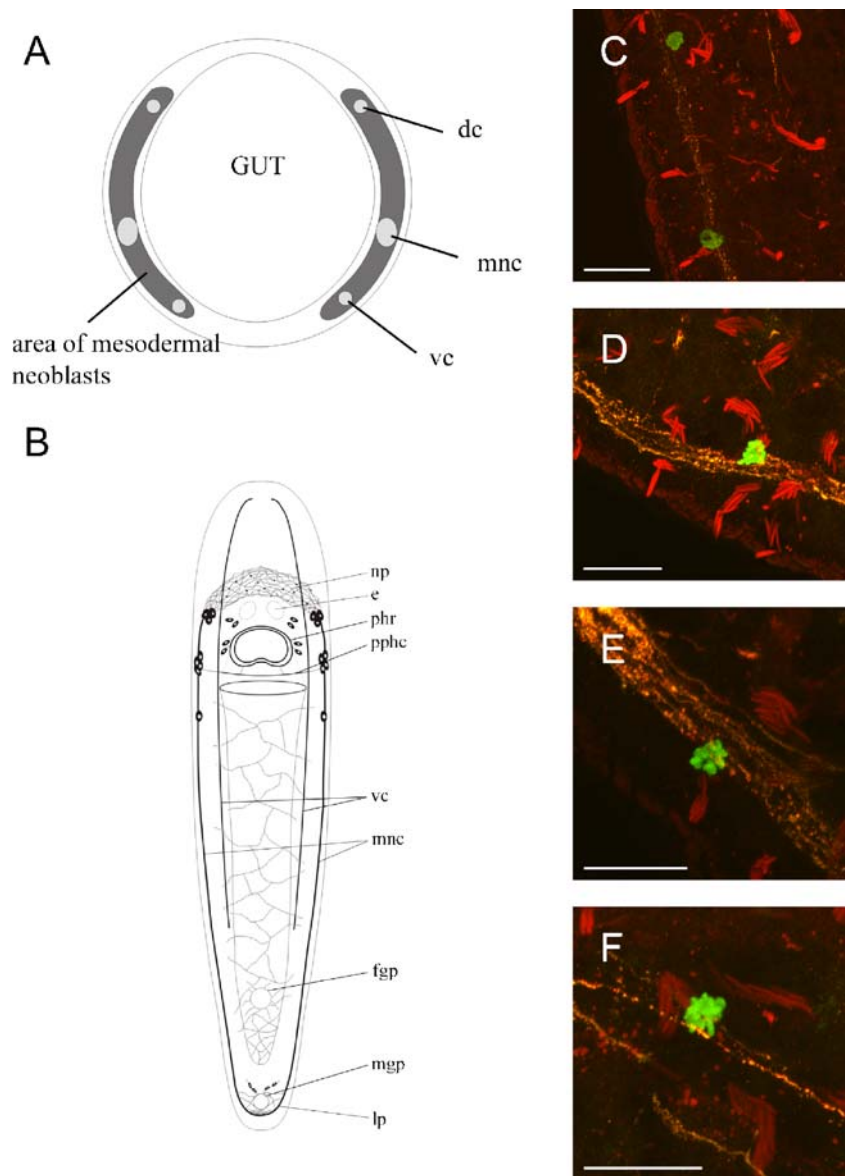
Discussion

Analysis of neoblasts at the ultrastructural level is essential for the correct identification of this cell type (see references in Palmberg 1990; Hori 1997; Hori et al. 1999; Rieger et al. 1999). Immunogold labeling of incorporated nucleotide analogs (used for the first time in this taxon) allows the distinction of S-phase and non-S-phase neoblasts and thus provides a better understanding of the dynamics of this cell system.

Location of neoblast populations

Most authors consider that platyhelminth neoblasts represent a permanent self-renewing pool forming a possibly totipotent stem cell system that produces all somatic and proliferating cells (Shibata et al. 1999; Peter et al. 2001; Saló and Bagaña 2002). Our data from adult animals support the presence of at least two somatic (mesodermal and gastrodermal neoblasts) and two gonadal (located in the testes and the ovaries) proliferating cell populations. For *M. hystricinum marinum*, Rieger et al. (1999) have indicated the similarity of the nuclear morphology of oogonia, spermatogonia, and stage 1 and stage 2 neoblasts. This supports the notion that germ cells and somatic neoblasts are derived from a single stem cell population. Bagaña and Boyer (1990) and Peter et al. (2001) have summarized evidence for somatic neoblasts entering the germ line in platyhelminths, particularly in planarians (absence of a separate traceable germ line, total reduction of gonads, repopulation of germ line after starvation,

Fig. 8 **a** Representation of a cross section of *M. lignano* showing the location of the dorsal (*dc*), main (*mnc*), and ventral (*vc*) cords (dark gray area two lateral bands of the area with mesodermal neoblasts). **b** Representation of the FMRF-amidergic nervous system (*e* eyes, *fgp* female genital pore, *lp* caudal loop, *mgp* male genital pore, *mnc* main lateral nerve cord, *np* nerve plexus, *phr* pharyngeal nerve ring, *pphc* postpharyngeal commissure, *vc* ventral nerve cord). **c-f** Laser scanning projections of FMRF-amide (red-orange) and H3 (green) double-stained *M. lignano*. Note the close vicinity of mitotic figures and the main nerve cord (red rods background staining of rhabdites). Bars 20 μ m



sexualization of asexual strains). Commenting on the experiments by Gremigni (1981, 1988), Saló and Bagaña (2002) have argued that undifferentiated cells committed to becoming germ cells can apparently be transformed into somatic cells. However, additional experiments (using genetically or cytologically marked neoblasts) will be needed to show the actual transformation of somatic neoblasts into germ cells (or vice versa) and the putative transformation of embryonic proliferating cells into post-embryonic neoblasts.

Ultrastructural stages of neoblasts, cell cycle, and differentiation

Changes in the arrangement and condensation of chromatin during the course of S-phase and differences in the location of DNA replication during early, middle, and late stages of S-phase have been reported (e.g., Mazzotti et al. 1998). A

similar result has been reported after the application of two different halogenated deoxyuridines, each with a different exposure time (Jaunin et al. 1998). Mazzotti et al. (1998) also suggest that chromatin becomes more condensed with the progression of S-phase. A different view has been proposed following analyses of interphase chromosome territories (Cremer and Cremer 2001; Tanabe et al. 2002).

The immunogold labeling of S-phase cells in this study allows a search for a correlation of nuclear fine structure and progression in S-phase. Chromatin condensation has been estimated by comparing the change of small condensed areas (stage 1) into larger ones (stage 3). Of all S-phase cells observed in our study, 79% correspond to the stages 2 or 2–3, the remaining cells (21%) being identified as stage 3 neoblasts. If chromatin condensation is seen as a measure of S-phase progression, the majority of S-phase neoblasts in our experiments would have been present in early to middle S-phase.

If we assume that changes in chromatin condensation occur during S-phase progression, we must interpret our observations of unlabeled neoblasts, of which 67% are stage 3 and only 8% stage 2, as showing that the majority of these neoblasts are post S-phase. The ultrastructure of nuclei from neoblasts of *M. hystricinum marinum* also shows significant morphological differences in chromatin structure (an increase in condensation from stage 1 to stage 3) that can be interpreted as stages; originally, these were not correlated with cell-cycle phases (Rieger et al. 1999).

From the present data, we cannot exclude that the nuclear and cytoplasmic differences of the neoblast stages observed so far (Rieger et al. 1999; this paper) are, in part, stages of sequential subpopulations of progenitor cells, each having different cell cycle characteristics (e.g., totipotent stem cells and various progenitor cells; see Peter et al. 2001, 2004). The presence of subtypes of neoblasts has been discussed for planarians (see references in Ladurner et al. 2000) and has been suggested based on specific staining (Schürmann et al. 1998) and quantitative video microscopy (Behensky et al. 2001). In particular, the increase of cytoplasmic specialization from stage 1 to stage 3 neoblasts may be taken as evidence for the presence of sequential subpopulations.

Further immunogold analysis of the neoblast compartment in *M. lignano* may show that our preliminary staging system of neoblasts is too general. Our two explanations for the observed differences in neoblast fine structure (different subpopulations or progression through S-phase) may indeed be combined. We believe that the data presented here open up a new avenue of investigations with respect to this proliferating cell system of platyhelminths.

Irrespective of the question as to whether the observed differences in neoblast structure are viewed as S-phase progression or different neoblast populations, we wish to point out that stage 3 neoblasts comprise the main fraction of all neoblasts (Table 1). We have obtained evidence that stage 3 neoblasts are migratory. A detailed analysis of apoptosis and of epidermal cell replacement has shown that differentiation of a stage 3 neoblast into an epidermal cell occurs close to the target tissue (Nimeth et al. 2002). The transcription of tissue-specific genes may occur earlier (Agata 2001).

Stage 1 neoblasts are not found in adult *M. lignano*. We have described such neoblasts in hatchlings and juveniles of *M. hystricinum marinum*. Stage 1 neoblasts have also been identified in regenerating animals (data not shown) and in hatchlings of *M. lignano*. Neoblasts with a similar nuclear and cytoplasmic structure as our stage 1 types are well known in planarians (e.g., Pedersen 1959; Morita et al. 1969; Hay and Coward 1975).

Total number of neoblasts

Only 6.5% (1600) of the total number of cells are somatic neoblasts in *M. lignano*. Previously published data on the total number of neoblasts in various planarian species have

been based on light-microscopic observations and are markedly higher than the number found in *M. lignano*. At least 30% of the total cell count have been classified as neoblasts (Baguña and Romero 1981; Peter 1995). These results need reinterpretation, as light microscopy is not sufficient for an unequivocal diagnosis of a neoblast (Hay and Coward 1975; Rieger et al. 1999).

However, neoblasts may indeed be more numerous in planarians, because of their remarkable regenerative powers (Saló and Baguña 2002) and the often truly exceptional modes of asexual reproduction (Peter et al. 2001). *M. lignano* reproduces solely sexually and has limited regenerative capacity (Salvenmoser et al. 2001). A comparison of quantitative ultrastructural data from microturbellarians that reproduce asexually (*Microstomum* sp., *Convolutriloba* sp.) might substantiate the correlation of high numbers of neoblasts and asexual reproduction. This is suggested by data from *Convolutriloba longifissura* in which S-phase neoblasts make up over 15% of all cells (Gschwentner et al. 2001).

Arrested neoblasts

In this paper, we report the presence of non-labeled stage 2 neoblasts after 1 week or 2 weeks of continuous BrdU exposure. Nimeth et al. (2004) have shown that at least 2% of all somatic neoblasts do not enter S-phase within 48 h. Light-microscopic data have clearly revealed that a significant proportion of neoblasts arrested in G2 is present in *Schmidtea mediterranea* (Baguña 1976; Saló and Baguña 1984). However, this has been contradicted by recent studies with BrdU and mitosis labeling (Newmark and Sánchez Alvarado 2000). For a final interpretation of the number of arrested neoblasts, our qualitative data presented here will have to be supplemented by quantitative counts.

Close spatial association of neoblasts and nervous system in *Macrostomum*

The close association of mesodermal neoblasts in S-phase with the nervous system in *Macrostomum lignano* is remarkable. BrdU pulses (30 min) have revealed two lateral bands of S-phase cells along the main nerve cords (Ladurner et al. 2000), restricted ventrally and dorsally by the ventral and dorsal nerve cord (Rieger et al. 1994; present study). We have found 69% of labeled neoblasts, 54% of all neoblasts (both from TEM analysis), and nearly all mitoses (from double staining of mitotic figures and neurotransmitters) in direct contact or within a distance of 5 μ m from the main ventrolateral nerve cords. Double staining of mitotic figures and neurotransmitters has further indicated the close association of mitotic figures with other parts of the nervous system (Fig. 8). Finally, the arrest of mitosis with colchicine and the specific staining of mitotic cells have demonstrated their position along the lateral margins bordered by the ventral and dorsal nerve cords (Ladurner et al. 2000). Therefore, the nervous system

might exert a guiding function on neoblasts via cell-cell connections or via neurosecretion, as proposed by Baguña et al. (1989). Our structural evidence in *Macrostomum* seems to support this suggestion.

Acknowledgements We thank Gunde Rieger and Robert Gschwentner for rewarding discussions.

References

- Agata K (2001) The regeneration system of planarians. *Belg J Zool* 131:101
- Baguña J (1976) Mitosis in the intact and regenerating planarian *Dugesia mediterranea* n. sp. I. Mitotic studies during growth, feeding and starvation. *J Exp Biol* 195:53–64
- Baguña J (1981) Planarian neoblasts. *Nature* 290:14–15
- Baguña J (1998) Planarians. In: Ferretti P, Géraudie J (eds) Cellular and molecular basis of regeneration: from invertebrates to human. Wiley, Chichester, pp 135–166
- Baguña J, Boyer BC (1990) Descriptive and experimental embryology of the Turbellaria: present knowledge, open questions and future trends. In: Marthy HJ (ed) Experimental embryology in aquatic plants and animals. Plenum, New York, pp 95–128
- Baguña J, Romero R (1981) Quantitative analysis of cell types during growth, degrowth and regeneration in the planarians *Dugesia mediterranea* and *Dugesia tigrina*. *Hydrobiologia* 84:181–194
- Baguña J, Saló E, Romero R (1989) Effects of activators and antagonists of the neuropeptides substance P and substance K on cell proliferation in planarians. *Int J Dev Biol* 33:261–266
- Behensky C, Schürmann W, Peter R (2001) Quantitative analysis of turbellarian cell suspensions by fluorescent staining with acridine orange, and video microscopy. *Belg J Zool* 131:131–136
- Best JB, Rosenfold R, Souders J, Wade C (1965) Studies on the incorporation of isotopically labeled nucleotides and amino acids in planaria. *J Exp Zool* 159:397–403
- Brøndsted H (1969) Planarian regeneration, Pergamon, Oxford
- Cremer T, Cremer C (2001) Chromosome territories, nuclear architecture and gene regulation in mammalian cells. *Nat Rev Genet* 2:292–301
- Ehlers U (1995) The basic organization of the Plathelminthes. *Hydrobiologia* 305:21–26
- Eisenman EA, Alfert M (1982) A new fixation procedure for preserving the ultrastructure of marine invertebrate tissues. *J Microsc* 125:117–120
- Gremigni V (1981) The problem of cell totipotency, dedifferentiation and transdifferentiation in Turbellaria. *Hydrobiologia* 84:171–179
- Gremigni V (1988) Planarian regeneration: an overview of some cellular mechanisms. *Zool Sci* 5:1153–1163
- Gschwentner R, Ladurner P, Nimeth K, Rieger R (2001) Stem cells in a basal bilaterian. S-phase and mitotic cells in *Convolutriloba longifissura* (Acoela, Platyhelminthes). *Cell Tissue Res* 304:401–408
- Gustafsson MKS (1976) Studies on cytodifferentiation in the neck region of *Diphyllbothrium dendriticum* Nitzsch, 1824 (Cestoda, Pseudophyllidae). *Z Parasitenk* 50:323–329
- Gustafsson MKS (1990) The cells of a cestode—*Diphyllbothrium dendriticum* as a model in cell biology. In: Gustafsson MKS, Reuter M (eds) The early brain. Åbo Academy Press, Åbo, pp 13–44
- Hacker GW, Muss WH, Hauser-Kronberger C, Danscher G, Rufner R, Gu J, Su H, Andreasen A, Stoltenberg M, Dietze O (1996) Electron microscopical autometallography: immunogold-silver staining (IGSS) and heavy-metal histochemistry. *Methods* 10:257–269
- Hay ED, Coward SJ (1975) Fine structure studies on the planarian, *Dugesia*. I. Nature of the “neoblast” and other cell types in noninjured worms. *J Ultrastruct Res* 50:1–21
- Hori I (1997) Cytological approach to morphogenesis in the planarian blastema. II. The effect of neuropeptides. *J Submicrosc Cytol Pathol* 29:91–97
- Hori I, Kishida Y (1998) A fine-structural study of regeneration after fission in the planarian *Dugesia japonica*. *Hydrobiologia* 383:131–136
- Hori I, Hikosaka-Katayama T, Kishida Y (1999) Cytological approach to morphogenesis in the planarian blastema. III. Ultrastructure and regeneration of the acoel turbellarian *Convoluta naikaiensis*. *J Submicrosc Cytol Pathol* 31:247–258
- Jaunin F, Visser AE, Cmarko D, Aten JA, Fakan S (1998) A new immunocytochemical technique for ultrastructural analysis of DNA replication in proliferating cells after application of two halogenated deoxyuridines. *J Histochem Cytochem* 46:1203–1209
- Ladurner P, Rieger R, Baguña J (2000) Spatial distribution and differentiation potential of stem cells in hatchlings and adults in the marine platyhelminth *Macrostomum* sp.: a bromodeoxyuridine analysis. *Dev Biol* 226:231–241
- Ladurner P, Schärer L, Rieger RM (2005) A new model organism among the lower Bilateria and the use of digital microscopy in taxonomy of meiobenthic Platyhelminthes: *Macrostomum lignano*, n. sp. (Rhabditophora, Macrostomorpha). *J Zool Sys Evol Res* 43:114–126
- Mazzotti G, Gobbi P, Manzoli L, Falconi M (1998) Nuclear morphology during the S Phase. *Microsc Res Tech* 40:418–431
- Morita M (1995) Structure and function of the reticular cell in the planarian *Dugesia dorotocephala*. *Hydrobiologia* 305:189–196
- Morita M, Best JB, Noel J (1969) Electron microscopic studies of planarian regeneration. I. Fine structure of neoblasts in *Dugesia dorotocephala*. *J Ultrastruct Res* 27:7–23
- Morrison SJ, Shah NM, Anderson DJ (1997) Regulatory mechanisms in stem cell biology. *Cell* 88:287–298
- Newmark PA, Sánchez Alvarado A (2000) Bromodeoxyuridine specifically labels the regenerative stem cells of planarians. *Dev Biol* 220:142–153
- Nimeth K, Ladurner P, Gschwentner R, Salvenmoser W, Rieger R (2002) Cell renewal and apoptosis in *Macrostomum* sp. [Lignano]. *Cell Biol Int* 26:801–815
- Nimeth KT, Mahlknecht M, Mezzanato A, Peter R, Rieger R, Ladurner P (2004) Stem cell dynamics during growth, feeding and starvation in the basal flatworm *Macrostomum* sp. (Platyhelminthes). *Dev Dyn* 230:91–99
- Palmberg I (1986) Cell migration and differentiation during wound healing and regeneration in *Microstomum lineare* (Turbellaria). *Hydrobiologia* 132:181–188
- Palmberg I (1990) Stem cells in microturbellarians: an autoradiographic and immunocytochemical study. *Protoplasma* 158:109–120
- Palmberg I, Reuter M (1983) Asexual reproduction in *Microstomum lineare* (Turbellaria). I. An autoradiographic and ultrastructural study. *Int J Inv Repr* 6:197–206
- Pedersen KJ (1959) Cytological studies on planarian neoblasts. *Z Zellforsch* 50:799–817
- Peter R (1995) Regenerative and reproductive capacities of the fissiparous planarian *Dugesia tahitiensis*. *Hydrobiologia* 305:261
- Peter R (2001) Experimentelle Systeme zum Studium von Regenerationsvorgängen: Turbellarien als Modellorganismen mit einem Stammzellensystem. *Ber Nat-Med Verein Innsbruck* 88:287–350
- Peter R, Ladurner P, Rieger RM (2001) The role of stem cell strategies in coping with environmental stress and choosing between alternative reproductive modes: turbellaria rely on a single cell type to maintain individual life and propagate species. *Mar Ecol—PSZNI* 22:35–51
- Peter R, Gschwentner R, Schürmann W, Rieger RM, Ladurner P (2004) The significance of stem cells in free-living flatworms: one common source for all cells in the adult. *J Appl Biomed* 2:21–35

- Reuter M, Kreshchenko N (2004) Flatworm asexual multiplication implicates stem cells and regeneration. *Can J Zool* 82:334–356
- Rieger RM, Gehlen M, Haszprunar G, Holmlund M, Legniti A, Salvenmoser W, Tyler S (1988) Laboratory cultures of marine *Macrostomida* (Turbellaria). *Fortschr Zool* 36:525
- Rieger RM, Tyler S, Smith JPS, Rieger GE (1991) Platyhelminthes: Turbellaria. In: Harrison FW, Bogitsh BJ (eds) *Microscopic anatomy of invertebrates, platyhelminthes and nemertinea*. Wiley-Liss, New York, pp 7–140
- Rieger RM, Salvenmoser W, Legniti A, Tyler S (1994) Phalloidin-rhodamine preparations of *Macrostomum hystricinum marinum* (Platyhelminthes): morphology and postembryonic development of the musculature. *Zoomorphology* 114:133–147
- Rieger RM, Legniti A, Ladurner P, Reiter D, Asch E, Salvenmoser W, Schürmann W, Peter R (1999) Ultrastructure of neoblasts in microturbellaria: significance for understanding stem cells in free-living Platyhelminthes. *Invertebr Repr Dev* 35:127–140
- Salvenmoser W, Riedl D, Ladurner P, Rieger R (2001) Early steps in the regeneration of the musculature in *Macrostomum* sp. (Macrostomorpha, Platyhelminthes). *Belg J Zool* 131:105–109
- Saló E, Baguña J (1984) Regeneration and pattern formation in planarians. I. The pattern of mitosis in anterior and posterior regeneration in *Dugesia (G) tigrina*, and a new proposal for blastema formation. *J Embryol Exp Morphol* 83:63–80
- Saló E, Baguña J (2002) Regeneration in planarians and other worms: new findings, new tools, and new perspectives. *J Exp Zool* 292:528–539
- Sánchez Alvarado A, Newmark PA, Robb SMC, Juste R (2002) The *Schmidtea mediterranea* database as a molecular resource for studying platyhelminthes, stem cells and regeneration. *Development* 129:5659–5665
- Sauzin-Monnot MJ (1973) Ultrastructural study of the *Dendrocoelum lacteum* neoblast during regeneration. *J Ultrastruct Res* 45:206–222
- Schärer L, Ladurner P (2003) Phenotypically plastic adjustment of sex allocation in a simultaneous hermaphrodite. *Proc R Soc Lond [Biol]* 270:935–941
- Schärer L, Ladurner P, Rieger RM (2004) Bigger testes are more active: experimental evidence that testis size reflects testicular cell proliferation activity in the marine invertebrate, the free-living flatworm *Macrostomum* sp. *Behav Ecol Sociobiol* 56:420–425
- Schürmann W, Betz S, Peter R (1998) Separation and subtyping of planarian neoblasts by density-gradient centrifugation and staining. *Hydrobiologia* 383:117–124
- Shibata N, Umesono Y, Orii H, Sakurai T, Watanabe K, Agata K (1999) Expression of vasa (*vas*)-related genes in germline cells and totipotent somatic stem cells of planarians. *Dev Biol* 206:73–87
- Smith AG, McKerr G (2000) Tritiated thymidine ([³H]-TdR) and immunocytochemical tracing of cellular fate within the asexually dividing cestode *Mesocostoides vogae* (syn. *M. corti*). *Parasitology* 121:105–110
- Spurr AR (1969) A low-viscosity epoxy resin embedding medium for electron microscopy. *J Ultrastruct Res* 26:31–45
- Tanabe H, Habermann FA, Solovei I, Cremer M, Cremer T (2002) Non-random radial arrangements of interphase chromosome territories: evolutionary considerations and functional implications. *Mutat Res* 504:37–45
- Willms K, Merchant MT, Gomez M, Robert L (2001) *Taenia solium*: germinal cell precursors in tapeworms grown in hamster intestine. *Arch Med Res* 32:1–7